The Journal of Immunology

RESEARCH ARTICLE | OCTOBER 15 2005

Increase in Phagocytosis after Geldanamycin Treatment or Heat Shock: Role of Heat Shock Proteins[1] FREE

Virginia L. Vega; ... et. al

J Immunol (2005) 175 (8): 5280–5287.
https://doi.org/10.4049/jimmunol.175.8.5280

Increase in Phagocytosis after Geldanamycin Treatment or Heat Shock: Role of Heat Shock Proteins[1]

Virginia L. Vega and Antonio De Maio[2]

The response to injury is activated at the systemic and cellular levels. At the systemic level, phagocytosis plays a key role in controlling infections and clearing necrotic and apoptotic cells. The expression of heat shock proteins (Hsp), which is a well-conserved process, is a major component of cellular response to stress. This study investigated the relationship between Hsps and phagocytosis. An increase in the phagocytosis of opsonized bacteria particles and latex beads was observed upon incubation of murine macrophages with geldanamycin (GA), a specific inhibitor of the Hsp90 family of proteins. The effect of GA on phagocytosis was blocked by coincubation with inhibitors of transcription (actinomycin D) or translation (cycloheximide), suggesting that gene expression was required. Because expression of Hsps has been observed after GA treatment, the effect of heat shock on phagocytosis was investigated. Similar to GA treatment, heat shock resulted in an actinomycin D-sensitive elevation of phagocytosis, which suggests that Hsps are involved. The increase in phagocytosis after GA treatment was not due to increased binding of opsonized particles to their respective receptors on the macrophage surface or to elevated oxidative stress. However, it was correlated with a rapid polymerization of actin in proximity to the plasma membrane. These results suggest that Hsps play a role in the modulation of the phagocytic process, which is part of the stress response. ***The Journal of Immunology,*** **2005, 175: 5280–5287.**

The response to injury is a complex process that includes cellular and systemic components. The best-characterized cellular response to stress is the expression of heat shock proteins (Hsp).[3] These proteins are involved in the repair and stabilization of cellular processes affected by the insult. In particular, Hsps play a key role in the folding of stress-induced denatured polypeptides and in the solubilization of protein aggregates (1, 2). The expression of Hsps after a mild stress renders cells more resistant to subsequent insults, a phenomenon that has been coined stress tolerance (2, 3). Hsps also participate in basic cellular processes, including folding and translocation of newly synthesized polypeptides across membranes, disassembly of clathrin cages, and stabilization of nuclear receptors (2). Recently, Hsps have been shown to modulate the functions of APCs (4, 5). Treatment of cells with geldanamycin (GA), a specific inhibitor of the Hsp90 family (6), is a common experimental approach to evaluating the role of Hsp90 in specific cellular processes. In addition, GA treatment results in induction of Hsps because heat shock factor-1 (HSF-1), which activates the transcription of these genes, is associated with Hsp90 under nonstressed conditions. Upon stress or after GA treatment, the HSF-1/Hsp90 complex dissociates, and HSF-1 is phosphorylated, trimerized, and translocated into the nucleus, where it activates the transcription of genes encoding for Hsps (7, 8).

The systemic response to injury is mediated by the activation of the hypothalamic-pituitary-adrenal and sympatho-adrenal-medullary axes, resulting in the induction of an inflammatory response (9, 10). The inflammatory process is characterized by the release of cytokines, chemokines, and lipid mediators, which trigger a cellular response by interacting with surface receptors on target cells (11). Binding to their specific receptors results in activation of a signal transduction pathway that ultimately allows the expression of other genes involved in the inflammatory and repair processes and in homeostasis restoration. Thus, the expression of these surface receptors may also be modulated by the stress response in an attempt to cope with the environmental changes imposed by the alteration of normal conditions. Professional phagocytes, such as macrophages (Mϕs), monocytes, dendritic cells, and polymorphonuclear leukocytes, play a key role in the development of inflammatory and immune responses. These cells actively participate in the clearance and neutralization of infective agents, necrotic cells, and apoptotic cells and in the synthesis of mediators that modulate the stress response. Phagocytosis is initiated by the recognition of foreign particles or apoptotic cells by specific receptors on the cell surface. For example, IgG-opsonized particles bind to FcγR on the Mϕ surface, resulting in the engulfment and internalization of the ligands. Phagocytosis requires actin rearrangement (12) and activation of Src and Syk tyrosine kinases (13, 14), Rho GTPases (15), PI3K, and phospholipases A_2, C, and D (16–18). The engulfment of the phagocytic ligand is mediated by internalization of the plasma membrane, resulting in a vesicle called a phagosome, which is targeted to the lysosomal compartment for degradation (19, 20). The question that emerges is whether this phagocytic process is modulated by components of the cellular stress response, such as Hsps. In the present study we show an enhancement of phagocytosis after treatment of Mϕs with GA or after heat shock (HS), suggesting that Hsps modulate the phagocytic process.

Division of Pediatric Surgery, Johns Hopkins University School of Medicine, Baltimore, MD 21205

Received for publication March 4, 2005. Accepted for publication August 8, 2005.

The costs of publication of this article were defrayed in part by the payment of page charges. This article must therefore be hereby marked *advertisement* in accordance with 18 U.S.C. Section 1734 solely to indicate this fact.

[1] This work was supported by National Institutes of Health Grant GM50878 and the Garrett Research Foundation.

[2] Address correspondence and reprint requests to Dr. Antonio De Maio, Johns Hopkins University School of Medicine, 720 South Rutland Avenue, Ross 746, Baltimore, MD 21205. E-mail address: ademaio@jhmi.edu

[3] Abbreviations used in this paper: Hsp, heat shock protein; AcD, actinomycin D; DAPI, 4′,6-diamido-2-phenylindole hydrochloride; DPI, diphenylene iodonium; DTNB, 5-5′dithio-bis 2-nitro benzoic acid; Grp94, glucose-regulated protein 94; Hsc70, constitutive heat shock protein 70; GA, geldanamycin; HA, herbamycin A; HS, heat shock; HSF-1, heat shock factor-1; IS, intensity of signal; Mϕ, macrophage; NAC, *N*-acetylcysteine; O_2^-, superoxide anion; PFA, paraformaldehyde; RD, radicicol; ROS, reactive oxygen species; SF, serum free.

0022-1767/05/$02.00

Thus, this increase in phagocytic capacity may be related to a rapid clearance of pathogens and apoptotic cells after injury.

Materials and Methods

Reagents

Actinomycin D (AcD), *N*-acetylcysteine (NAC), diphenylene iodonium (DPI), 5-5′dithio-bis 2-nitro benzoic acid (DTNB), GA from *Streptomyces hygroscopicus*, MTT, and NBT were purchased from Sigma-Aldrich. FITC-labeled *Escherichia coli* (K-12) particles, *Staphylococcus aureus* (wood strain without protein A) particles, latex beads (2 μm diameter), BioParticle opsonizing reagent, and Alexa Fluor 532-conjugated phalloid toxin were purchased from Molecular Probes. Abs against Hsp90 (SPA-830), glucose-regulated protein 94 (Grp94) (SPA-850), constitutive heat shock protein 70 (Hsp70) (SPA-810), and Hsc70 (SPA-820) were purchased from StressGen Biotechnologies.

Cell culture conditions and treatments

The murine macrophage cell line J774A.1 was obtained from American Type Culture Collection and was cultured in RPMI 1640 medium supplemented with 10% heat-inactivated FBS, 10 IU/ml penicillin, and 10 μg/ml streptomycin at 37°C with 5% CO_2 in a humidified incubator. Cells were plated at least 16 h before the experiments. Cells were treated with GA (1 μg/ml) for up to 5 h at 37°C. HS was performed by incubation of the cells for 1.5 h at 42°C, followed by a recovery period at 37°C.

Phagocytosis assay and visualization of internalized particles

Particles were opsonized by incubation with commercial IgG for 0.5 h at 37°C. Cells (2×10^5/well) were incubated in RPMI 1640 complete medium for 16 h. Cells were washed twice with sterile PBS and incubated with serum-free (SF) medium (RPMI 1640 supplemented with 1% penicillin/streptomycin) for 0.5 h at 37°C. Phagocytosis was evaluated by incubation of cells with 50 μl of FITC-conjugated IgG-coated particles (70 μg/ml) for 2 h at 37°C. The medium was removed, and cells were washed twice with SF medium and PBS. To quench noninternalized signal, cells were incubated with trypan blue (1 min at 25°C). The intensity of the internalized signal (IS) was measured using a fluorometer (excitation, λ_{480} nm; emission, λ_{520} nm) and normalized by the number of live cells in each well as estimated by the MTT assay. Results were expressed as the phagocytic index (IS/MTT). To visualize phagocytosed particles, cells (0.5×10^6 on a glass cover slide) were subjected to the phagocytic procedure described above and fixed with 4% paraformaldehyde (PFA) for 10 min at 25°C. Slides were mounted using 3.9% 1,4-diazabicyclo[2,2,2]octane in permaFluor aqueous mounting medium in the presence of trypan blue and visualized using a fluorescent microscope.

Immunostaining and F-actin visualization

Cells (0.5×10^6 cells/slide) were fixed with 4% PFA and permeabilized (when indicated) with cold acetone (15 s). Nonspecific binding was blocked by incubation with 30% human serum, 0.1% BSA, 1% fish gelatin, 5 mM EDTA, and 0.2% Tween 20 in PBS for 0.5 h at 4°C. Cells were incubated with primary Abs (1/200 dilution) for 1 h at 4°C, extensively washed with 30% FBS and 0.2% Tween 20 in PBS, and incubated with secondary Abs (1/1000 dilution) for 0.5 h at 4°C. Nuclei were stained with 4′,6-diamido-2-phenylindole hydrochloride (DAPI; 15 s, 25°C), and cells were visualized using a fluorescent microscope. The presence of F-actin was detected in acetone-permeabilized cells by incubating with Alexa Fluor 532-conjugated phalloid toxin (1/1000) for 0.5 h at 4°C.

Quantification of F-actin formation

F-actin formation was quantified by detecting the bound signal of Alexa Fluor 532-conjugated phalloid toxin as previously described (21). J774 cells (1×10^6 cells/glass cover slide) were fixed in 3.7% formalin and 1% Triton X-100 (10 min, 25°C), followed by incubation with 0.2 μM Alexa Fluor 532-conjugated phalloid toxin (30 min, 25°C). Cells were washed extensively with PBS and incubated with 2 μg/ml DAPI (10 min, 25°C). F-actin-bound fluorescent phalloid toxin was extracted with 300 μl of methanol, and the IS of both Alexa Fluor 532 (excitation, λ_{525} nm; emission, λ_{550} nm) and DAPI (excitation, λ_{355} nm; emission, λ_{458} nm) were measured by fluorometry. The values for F-actin were normalized by the DAPI signal.

FcγR quantification by flow cytometry

One million cells were fixed in 1% PFA and incubated with FITC-conjugated CD16/CD32 Ab (1/200 dilution) for 1 h at 4°C. Cells were analyzed using a FACSort and CellQuest software (BD Biosciences).

Western blotting

Cells were washed twice with cold 50 mM β-glycerol phosphate (pH 7.3) (containing 1.5 mM EGTA, 1.0 mM EDTA, 0.1 mM sodium vanadate, 1.0 mM benzamide, and 2 μg/ml pepstatin A), scraped, lysed in 300 μl of 20 mM Tris-HCl (pH 7.4) (containing 137 mM NaCl, 10% glycerol, 0.1% SDS, 0.5% deoxycholate, 1% Triton X-100, 2.0 mM EDTA, 4 mg/ml trypsin inhibitor, 1 mg/ml benzamide, 5 μmol/ml leupeptin, 200 μM sodium vanadate, 100 nM okadaic acid, and 1 mg/ml PMSF), for 0.5 h at 4°C, and centrifuged (15 min, 5800 rpm at 4°C). The protein concentration in the supernatant was determined by the bicinchoninic acid method (Pierce). Total proteins (50 μg) were separated by SDS-PAGE and transferred onto a nitrocellulose membrane (400 mA for 3 h). Membranes were blocked with 5% nonfat milk/3% BSA in TBS (pH 7.4) for 1 h at 25°C. Primary Abs (1/5000 dilution in TBS) were incubated for 16 h at 4°C. Membranes were rinsed twice with washing solution (0.3% Tween 20 and 0.05% Nonidet P-40 in TBS; pH 7.4), and incubated with HRP-conjugated secondary Abs (1/25,000 in TBS) for 2 h at 4°C. Proteins were detected using the SuperSignal chemiluminescent detection kit (Pierce).

Northern blotting

Total RNA was isolated using 1 ml of TRIzol reagent (Invitrogen Life Technologies). RNA (10 μg) was separated in formaldehyde-agarose gels and transferred onto a nylon-modified membrane (GeneScreen Plus; PerkinElmer). Blots were hybridized at 42°C with a cDNA probe radiolabeled by the random primer method (22) using [α-^{32}P]dATP and [α-^{32}P]dCTP, as previously described (23). Blots were washed twice at 42°C with washing solution I (6× SSC/1% SDS), followed by two washings with washing solution II (2× SSC/0.1% SDS). The signal was detected using the Molecular Dynamics phosphor screen system (3 h).

Superoxide anion ($O_2^{\cdot -}$) production (NADPH oxidase activity)

Detection of $O_2^{\cdot -}$ was performed by incubating J774 cells (1×10^6) for 1 h at 37°C with 2% NBT dissolved in SF medium in the presence or the absence of 10 μM DPI, an NADPH oxidase inhibitor. Cells were washed twice with PBS, harvested in 500 μl of PBS, pelleted (2 min at 5000 rpm), and lysed with 100 μl of 50% acetic acid. Formazan suspensions were dissolved by sonication (15 s, 2 A), and absorbance was measured at 560 nm. Values were rectified by the protein content in each well. NADPH oxidase activity was expressed as percentage of total intracellular $O_2^{\cdot -}$ production and calculated as: NBT − (NBT + DPI).

Total thiol levels

Total thiol levels were determined as described by Ellman and Lysko (24). In brief, Mϕs (1×10^6) were treated with 250 μl of cold 6% TCA and centrifuged (5 min, 4°C, 5000 rpm). An aliquot of the supernatant (100 μl) was mixed with 2% Na_2HPO_4 and 0.04% DTNB, and absorbance was immediately measured at 412 nm. Values were rectified by protein content in each sample and expressed as a percentage of the value for control or untreated cells.

Results

Phagocytosis is enhanced upon treatment of murine Mϕs with GA, which depends on gene expression

Murine Mϕs (J774 cell line) were treated with GA (1 μg/ml) for 0–3 h, and phagocytosis was monitored by incubation with IgG-opsonized FITC-conjugated *S. aureus* particles (2 h at 37°C). Cells were washed extensively with PBS to remove nonphagocytosed particles and then were incubated with trypan blue to quench any remaining signal from noninternalized particles. Subsequently, the signal corresponding to internalized particles was measured using a fluorometer. An increase in phagocytosis (presented as the phagocytic index) was observed to be proportional to the time of GA treatment compared with nontreated cells ($t = 0$). Under these conditions, 95% of opsonized particles were internalized as detected by immunostaining with anti-IgG Ab. The increase in phagocytosis was reduced by coincubation with the transcription inhibitor AcD (Fig. 1*A*) or with the translation inhibitors (cycloheximide or purinomycin), suggesting that gene expression was required. Cells treated with AcD alone were not different from untreated cells (Fig. 1*A*). Alternatively, phagocytosis was visualized by fluorescent microscopy under the conditions described

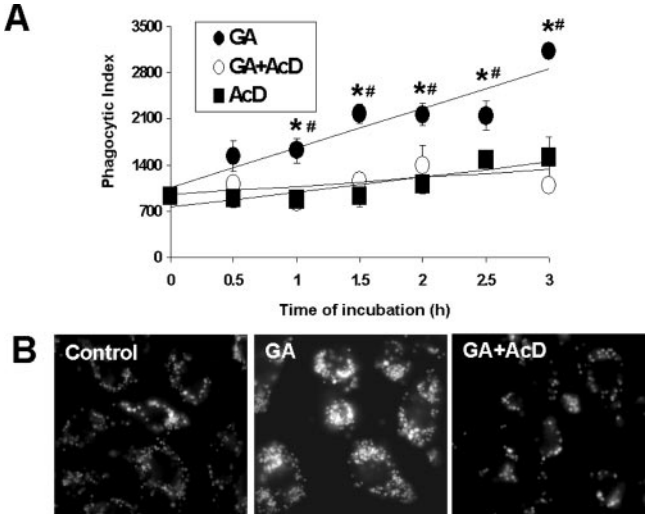

FIGURE 1. GA treatment resulted in an increase in phagocytosis that was sensitive to AcD. Cells (2×10^5) were incubated with SF medium (0.5 h, 37°C), followed by incubation with GA (1 μg/ml) for 0–3 h at 37°C. Then cells were incubated with FITC-conjugated *S. aureus* IgG-coated particles (70 μg/ml) in SF medium for 2 h at 37°C. Cells were extensively washed with PBS, and any remaining noninternalized signal was quenched by incubation with trypan blue for 1 min at 25°C. The internalized signal was measured by fluorometry (λ, 480–520 nm) and was normalized by the number of viable cells in each well as measured by MTT assay. Results are expressed as the phagocytic index (IS/MTT). Cells were incubated in parallel with GA (1 μg/ml) and AcD (10 μg/ml) or with AcD alone, and phagocytosis was measured as described above (*A*). Statistical analysis was performed by one-way ANOVA, followed by Newman-Keuls test. *, $p < 0.05$ vs untreated cells (time zero); #, $p < 0.05$ vs GA- plus AcD-treated or AcD-treated cells. Alternatively, phagocytosis was visualized by fluorescent microscopy after 3 h of incubation with GA, AcD, or GA plus AcD (*B*).

above, confirming the preceding observations (Fig. 1*B*). The same enhancing effect of GA on phagocytosis was observed for opsonized (IgG or fresh human serum) *E. coli* particles or latex beads. Other Hsp90 inhibitors, such as herbamycin A (HA) and radicicol (RD), reproduced the AcD-sensitive increase in phagocytosis observed with GA (data not shown). Phagocytosis of nonopsonized bacterial particles or latex beads increased after GA treatment, although this increase was smaller than that observed for opsonized particles. Thus, the GA-associated increase in phagocytosis was observed at different concentrations of phagocytic ligands and after different periods of incubation with opsonized particles (data not shown). Finally, other Mϕ lines, such as Raw.264 and ANA-1, displayed the same effect of GA on phagocytosis as J774 cells (data not shown). Hence, the effect of GA on phagocytosis appears to be a general event that is independent of ligand or grade/type of opsonization and requires gene expression.

Increase in phagocytosis after GA treatment correlates with expression of Hsps

The preceding observations suggest that gene expression is required for the effect of GA on phagocytosis. Hsps are expressed after GA treatment because Hsp90 is a negative regulator of HSF-1 (7, 25, 26). To document that indeed treatment with GA under our working conditions induced the expression of Hsps, we followed the appearance of Hsp70, the inducible member of the Hsp70 family. Hsp70 expression is the most appropriate and sensitive marker of the HS response, because this gene is not expressed in nonstress conditions. Cells (J774) were incubated with GA (1 μg/ml) for 1, 3, and 5 h. An increase in Hsp70 mRNA levels was observed within 1 h of GA treatment (Fig. 2*A*), followed by the appearance of the protein between 3 and 5 h of treatment (Fig. 2*B*). No detectable levels of Hsp70 were observed when cells were treated with GA in the presence of AcD (data not shown). In contrast, GA treatment did not significantly alter the expression of Hsp90, probably due to the great abundance of this protein (Fig. 2*B*). Neither Grp94 nor Hsc70 levels were increased after GA treatment, which is consistent with the fact that these genes are not induced by HSF-1. Moreover, levels of β-actin were not affected during GA treatment (Fig. 2*B*). Detection of Hsp70 by immunostaining indicated the appearance of Hsp70 in close proximity to cellular membranes (Fig. 2*C*). Hsp70 did not colocalize with calnexin (an endoplasmic reticulum marker), GM130 (a *trans*-Golgi marker) or transferrin (an early/recycling endosome marker; data not shown). Thus, these results suggest that GA treatment indeed induces Hsp70, as previously established (7, 25–27).

HS also enhances phagocytosis of IgG-coated particles

If Hsps play a role in the regulation of phagocytosis, it would be expected that their induction by hyperthermia would result in an increase in phagocytosis. Thus, J774 cells were thermally stressed at 42°C for 1.5 h and recovered at 37°C for 3, 6, and 24 h. The phagocytosis assay was performed as described above, using FITC-conjugated *E. coli* IgG-coated particles (2 h at 37°C). Our results showed an increase in phagocytosis after HS (Fig. 3), which was blocked by the presence of AcD during HS (Fig. 3*B*), indicating that gene expression was also required for the increase in phagocytosis following the stress. Binding of opsonized particles to the Mϕ surface without significant internalization was observed immediately after HS treatment (Fig. 3*A*). A small increase in phagocytosis was observed after a short recovery period following HS. This increase was also observed in cells incubated with AcD, suggesting that the effect may be related to hyperthermia rather than to Hsp expression (Fig. 3*B*). The small increase in phagocytosis could also be related to internalization of the particles that were bound, but not internalized, during HS (Fig. 3*A*). To evaluate

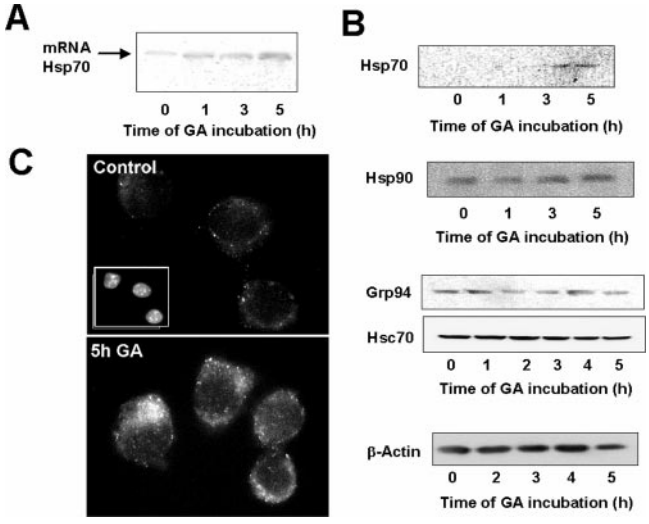

FIGURE 2. GA treatment resulted in an increase in Hsp70 expression. J774 cells were incubated with GA (1 μg/ml) for 0–5 h, and total RNA (6×10^6) was extracted and analyzed by Northern blotting for Hsp70 mRNA detection (*A*), or cells were lysed (6×10^6) for Western blot analysis of Hsp70, Hsp90, Grp94, Hsc70, and β-actin (*B*). Cells were incubated without (control cells) or with GA for 5 h and were permeabilized with acetone. The presence of Hsp70 was visualized using an anti-rabbit Hsp70 Ab (1/200, 1 h, 4°C), followed by FITC-conjugated Ab (1/1000, 0.5 h, 4°C) under a fluorescent microscope (*C*).

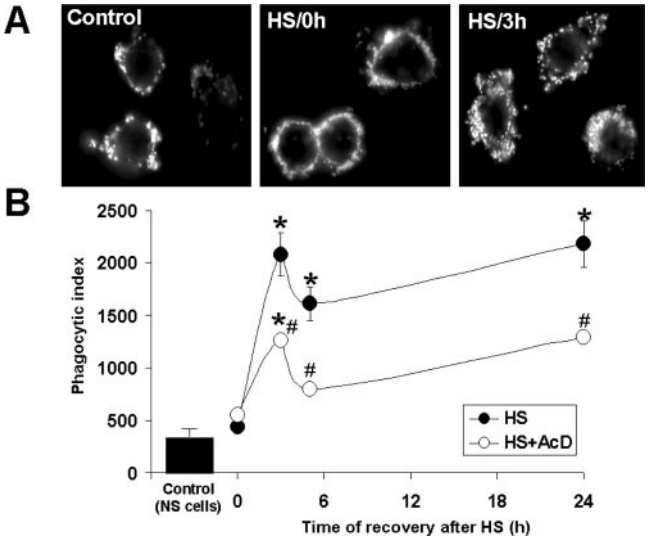

FIGURE 3. HS resulted in an increase in phagocytosis, which was sensitive to AcD. J774 cells were administered HS (42°C, 1.5 h) and allowed to recover at 37°C for 3, 6, or 24 h. AcD (10 μg/ml) was added at the beginning of HS and remained for 6 h during the recovery period. Phagocytosis was measured using FITC-conjugated *E. coli* IgG-coated particles. Internalization of opsonized particles was monitored by fluorescent microscopy at the end of the HS period (HS/0 h) or after HS and 3 h of recovery (HS/3 h; *A*) or was quantified using a fluorometer (*B*). The internalized signal was normalized by the number of viable cells in each well and was expressed as the phagocytic index (IS/OD MTT). Statistical analysis was performed by one-way ANOVA, followed by Newman-Keuls test. $*$, $p < 0.05$ vs untreated cells; #, $p < 0.05$ vs GA-treated cells.

whether the increase in phagocytosis after GA treatment and that after HS were due to the same mechanism, J774 cells were administered HS (42°C, 1.5 h), allowed to recover at 37°C for 24 h, and later treated with GA (1 μg/ml) for 1–4 h. There was a significant increase in IgG-coated particle phagocytosis after HS/24-h recovery compared with that in non-HS cells. However, phagocytosis was not further increased after subsequent treatment with GA (Fig. 4), suggesting that GA and HS modulate phagocytosis by a similar mechanism. In addition, the effect of GA is unlikely to be due to direct inhibition of Hsp90 function.

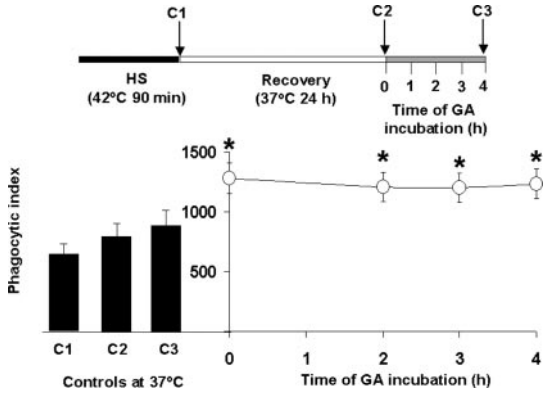

FIGURE 4. GA treatment after HS did not further enhance phagocytosis in J774 cells. Cells (2×10^5) were administered HS (42°C, 1.5 h) and allowed to recover for 24 h at 37°C. Cells were then treated with GA (1 μg/ml) for 1–4 h, and phagocytosis of FITC-conjugated *E. coli* IgG-coated particles was evaluated. Results are expressed as the phagocytic index (IS/OD MTT). Statistical analysis was performed by one-way ANOVA, followed by Newman-Keuls test. $*$, $p < 0.05$ vs untreated cells.

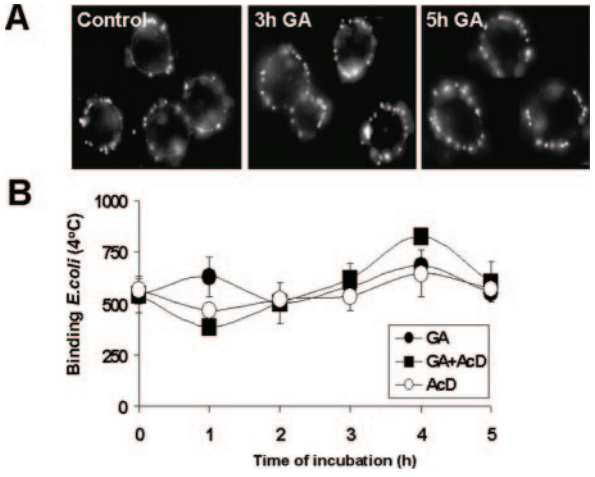

FIGURE 5. Binding of opsonized *E. coli* particles to Mϕ surface was not affected by GA treatment. J774.A1 cells were incubated in the absence or the presence of GA, GA plus AcD, or AcD for 1–5 h, followed by incubation for 0.5 h at 4°C. Cells were then incubated with prechilled FITC-conjugated *E. coli* IgG-coated particles for 1 h at 4°C. Cells were washed twice with cold PBS, and the presence of the opsonized particle was visualized using a fluorescent microscope (*A*) or was quantified by fluorometry (*B*). Values were normalized by the number of viable cells in each well as measured by the MTT assay, and results are expressed as *E. coli* binding at 4°C (IS/OD MTT). Statistical analysis was performed by one-way ANOVA, followed by Newman-Keuls test. $*$, $p < 0.05$ vs control or untreated cells.

Increase in phagocytosis after GA treatment is not due to an increase in binding of opsonized particles

To understand the possible mechanism involved in the increase in phagocytosis after GA treatment, we investigated whether binding of fluorescent IgG-opsonized particles to the Mϕ surface was modified after GA treatment. Cells (J774) were incubated with GA for

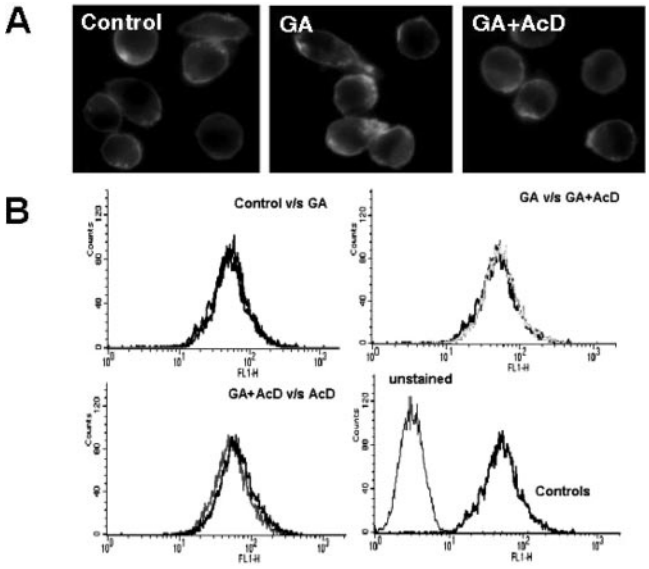

FIGURE 6. An increase in phagocytosis after GA treatment did not correlate with an increase in FcγR levels. J774 cells were incubated with GA (1 μg/ml), AcD (10 μg/ml), a combination of GA and AcD, or in the absence of any drug for 3 h. Detection of FcγRs was made by immunostaining in nonpermeabilized cells using anti-mouse CD16/CD32 Ab (1/200 dilution, 0.5 h, 4°C; *A*). Quantification of the cell surface expression of FcγRs was performed by FACS analysis (*B*).

0–5 h at 37°C, then incubated at 4°C with prechilled SF medium for 0.5 h and exposed to prechilled FITC-conjugated *E. coli* IgG-coated particles for 1 h at 4°C. Cells were washed at 4°C with cold PBS and fixed. Cell surface binding was visualized by fluorescent microscopy (Fig. 5*A*) or quantified using a fluorometer (Fig. 5*B*). No differences in particle binding to the cell surface were observed between untreated cells (control) or GA-treated cells within 5 h of incubation (Fig. 5). The addition of AcD (10 μg/ml) in the presence or the absence of GA did not alter the binding of FITC-conjugated IgG-coated particles at 4°C (Fig. 5*B*). To corroborate these observations, we evaluated the effect of GA treatment on the cell surface expression of FcγR, which is the receptor for opsonized IgG particles. No changes in receptor levels were detected by immunostaining (Fig. 6*A*) or FACS analysis (Fig. 6*B*) after GA treatment compared with control cells. Neither treatment of cells with AcD nor with the combination of AcD and GA modified the surface expression of FcγRs within 3 h of treatment. These observations suggest that the increase in phagocytosis after GA treatment is unlikely to be due to an elevation in the number of receptors on the cell surface.

Increase in phagocytosis observed after GA treatment is not due to an elevation in oxidative stress

Previous studies have shown that treatment of cells with GA results in the production of reactive oxygen species (ROS) and the activation of oxidative stress secondary to the metabolism of this drug via cytochrome P450 (28, 29). Thus, the effect of GA on phagocytosis could be due to early generation of ROS. To evaluate the effect of oxidative stress on the GA-induced increase in phagocytosis, cells were incubated (1–3 h, 37°C) with or without GA in the presence of NAC (1 mM). NAC is a precursor for reduced glutathione and a strong nonenzymatic antioxidant. The phagocytic assay was performed, as described above, using FITC-conjugated *E. coli* IgG-coated particles. GA treatment resulted in increased phagocytosis even in the presence of NAC (Fig. 7*A*), suggesting that oxidative stress does not factor into the GA effect. Treatment of cells with GA (1 μg/ml, 1–5 h) did not reduce nonenzymatic intracellular antioxidant capacity, measured as total thiol levels (Fig. 7*B*), indicating the lack of oxidative damage. Treatment of cells with RD, a nonquinone Hsp90 inhibitor, also resulted in an AcD-sensitive increase in phagocytosis, confirming that oxidative stress was not involved in this effect (Fig. 7*C*). Finally, activation of NADPH oxidase, which has been shown to occur during phagocytosis, was monitored. This enzyme is responsible for massive production of ROS in myeloid cells upon activation (30). J774 cells were incubated with or without GA (1 μg/ml, 3 h), medium was removed, and 0.2% NBT solution was added (1 h, 37°C) in the presence or the absence of DPI, an NADPH oxidase inhibitor. GA treatment alone did not result in a significant increase in NADPH oxidase activation compared with control or untreated cells (Fig. 7*D*). However, higher total $O^{\cdot}$ production was observed in GA-treated cells, probably due to cytochrome P450 metabolism of this drug (data not shown). The addition of IgG-coated latex beads resulted in a significant increase in NADPH oxidase activation, which was higher in GA-treated vs control cells (45 and 22% over basal levels, respectively). In summary, these results showed that the effect of GA on phagocytosis was unlikely to be due to changes in the redox status of Mϕs.

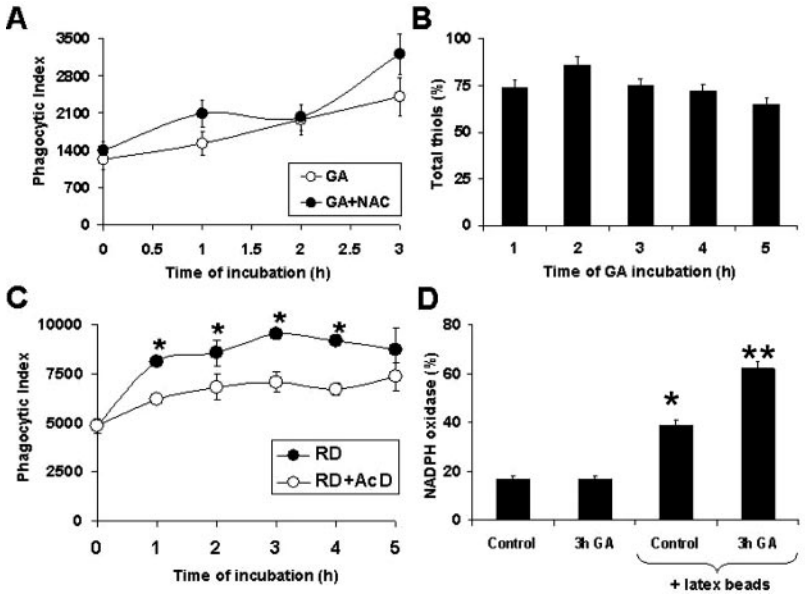

FIGURE 7. Oxidative stress did not correlate with a GA-induced increase in phagocytosis. *A*, Cells were incubated with GA (1 μg/ml) in the presence or the absence of NAC (1 mM) for 1–3 h and assayed for phagocytosis as described above. The internalized signal was normalized by the number of viable cells in each well as measured by the MTT assay, and results are expressed as the phagocytic index (IS/MTT). *B*, Total thiol levels were determined spectrophotometrically (412 nm) by addition of DTNB. The OD value was normalized by protein levels in each sample. Results are expressed as a percentage of the values for control (untreated) cells. *C*, Phagocytosis of FITC-conjugated IgG-coated *S. aureus* (70 μg/ml) particles was determined after treatment with RD (1 μg/ml), a nonquinone inhibitor of the Hsp90 family. *, $p < 0.05$ vs control or untreated cells and vs RD- plus AcD-treated cells. *D*, The percentage of NADPH oxidase activity was estimated by incubating cells with NBT in the presence or the absence of DPI, an inhibitor of NADPH oxidase. To evaluate the effect of IgG-coated ligands on its activation, cells were incubated for 1.5 h with latex beads (70 μg/ml) after NBT incubation. NBT oxidation by $O_2^{\cdot -}$ was monitored at 540 nm and normalized by the protein content in each sample. The percentage of NADPH activation was calculated by subtracting the NBT plus DPI value from the NBT value. Results are expressed as the activity of NADPH oxidase (percentage of total $O_2^{\cdot -}$ production). Statistical analysis was performed by one-way ANOVA, followed by Newman-Keuls test. *, $p < 0.05$ vs control or untreated cells; **, $p < 0.05$ vs latex bead-incubated cells.

An increase in actin polymerization is observed after GA treatment or HS

Actin polymerization is part of the mechanism associated with the internalization of particles by phagocytosis. We investigated whether treatment with GA or HS induced F-actin formation, as visualized using fluorescent-conjugated phalloid toxin. J774 cells were either incubated with GA (1 h) or subjected to HS (42°C, 3 h), fixed with 4% PFA, permeabilized with cold acetone, and incubated with Alexa Fluor 532-conjugated phalloid toxin (1/1000 dilution, 30 min). Very low levels of F-actin were observed in control cells. Both GA treatment and HS resulted in a significant increase in actin polymerization surrounding the plasma membrane (Fig. 8*A*). Actin polymerization after both GA treatment and HS was reduced by coincubation with AcD (10 μg/ml), although no F-actin formation was observed in the presence of AcD alone. These results suggest that actin polymerization is probably secondary to the expression of new genes (i.e., Hsps) after GA or HS treatment. To substantiate these findings, J774 cells were incubated with GA for different time periods, and F-actin levels were quantified as described in *Materials and Methods*. No differences in F-actin formation were observed between cells incubated for 15 min with GA or GA plus AcD compared with untreated (control) cells in the presence or the absence of phagocytic ligands (IgG-coated latex beads; Fig. 8*B*). This short period of incubation with GA did not result in a significant increase in Hsp70. When the treatment was prolonged for 1.5 h, an increase in actin polymerization was observed in GA-treated cells compared with cells coincubated with GA and AcD or untreated cells (Fig. 8*C*, time zero). The addition of IgG-coated latex beads to these treated cells resulted in an additional increase in F-actin levels, which was proportional to the prestimulation level (Fig. 8*C*). Thus, the kinetics of F-actin formation under these conditions (with or without coincubation with AcD) were also different from those observed in untreated cells after incubation with IgG-coated latex beads (Fig. 8*C*). Similar observations were made after treatment of cells with HA or RD (data not shown).

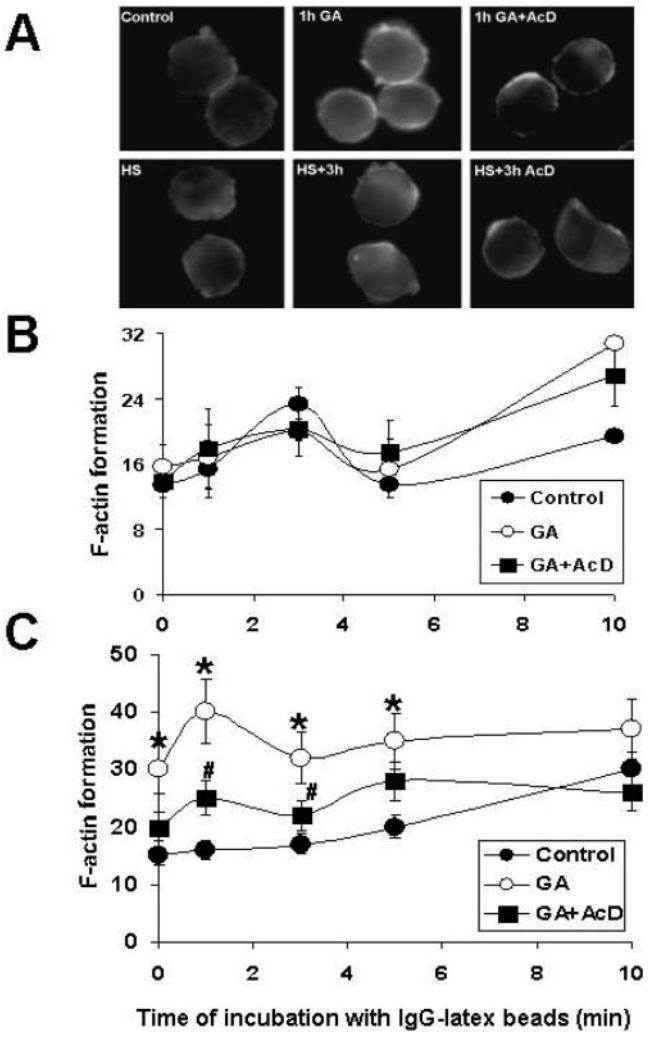

FIGURE 8. An increase in F-actin was observed after treatment with GA and after HS. *A*, J774.A1 cells on glass cover slides were treated with GA or HS (42°C, 1.5 h). Cells were fixed in PFA and permeabilized with cold acetone. Polymerized actin was detected by incubation with Alexa Fluor 532-conjugated phalloid toxin (1/1000 dilution, 30 min). Cells were treated with GA, GA plus AcD, or AcD alone for 1 h. Cells were HS and allowed to recover for 3 h at 37°C in the absence or the presence of AcD. Quantification of F-actin was performed using Alexa Fluor 532 phalloid toxin, as described in *Materials and Methods*. Cells were treated, or not (control), with GA or GA plus AcD for 15 min (*B*) or 1.5 h (*C*), followed by incubation with IgG-coated latex beads (70 μg/ml, 25°C). Results are expressed as F-actin formation (IS/DAPI). Statistical analysis was performed by one-way ANOVA, followed by Newman-Keuls test. *, $p < 0.05$ vs control or untreated cells; #, $p < 0.05$ vs GA-treated cells.

Discussion

Phagocytosis plays an important role under normal and pathological conditions. For example, apoptotic cells that appear as part of tissue remodeling are cleared by phagocytosis. Phagocytosis is also necessary for the rapid clearance of pathogens, necrotic tissue, and stress-induced apoptotic cells. The rapid clearance of foreign particles and damaged cells accelerates the repair process and reduces the activation of a secondary inflammatory response, thereby contributing to improved survival. Another component of the response to injury that improves survival is the expression of Hsps. Up until now, the relationship between phagocytosis and Hsp expression was not well documented. In the present study we showed increases in phagocytosis after HS and after GA treatment, both of which required gene expression. Thus, Hsps probably modulate the phagocytic process. It appears that these two conditions, GA treatment and HS, follow the same mechanism, because their combination did not result in an additive or synergistic effect on phagocytosis. Previous studies have suggested that the effects of GA may be mediated by oxidative stress, because this molecule, which contains a quinone group, is metabolized by the cytochrome P450 complex, thereby generating ROS (28). We observed a similar increase in phagocytosis upon incubation with HA and RD, which are also inhibitors of Hsp90. Because RD lacks the quinone group, it is unlikely that the effect of Hsp90 inhibition on phagocytosis is mediated by the activation of oxidative stress.

Phagocytosis is initiated by the recognition of foreign particles or damaged cells by specific receptors on the Mϕ surface. This initial event is followed by the engulfment and internalization of the ligand by plasma membrane-derived structures, which are sealed into vesicles called phagosomes. These phagosomes undergo a maturation process characterized by interaction with the endosomal compartment and targeting to lysosomes. Our results showed Hsp70 in close proximity to the plasma membrane and in vesicle-like structures upon treatment with GA. The subcellular localization of Hsp70 after GA treatment was not completely identical with that observed after HS, which displayed a more diffuse pattern, although membrane staining has been observed (31). The major difference between HS and GA treatment is the appearance during HS of denatured polypeptides, the natural substrates for

Hsp70. In contrast, GA does not induce massive amounts of unfolded polypeptides, leaving Hsp70 free to interact with other cellular targets, such as membranes. In support of this assumption, early studies have shown that Hsp70 is capable of interacting with membrane lipids (32). Recently, Hsp70 was shown to interact with phosphatidylserine with high specificity (33). This lipid is a major component of the cytosolic side of cellular membranes. Although Hsp70 is a strong candidate to mediate the enhancement of phagocytosis after GA treatment or HS, we cannot discard the possibility that other proteins induced during these conditions are involved.

Formation of the phagosome is driven by actin polymerization. We have also observed an increase in F-actin in close proximity to the plasma membrane after HS or GA treatment in the absence of phagocytic ligands. Detection of F-actin in cells treated with GA was elevated compared with that in control cells and was reduced by coincubation of GA with AcD, suggesting that a molecule(s) expressed after GA treatment may trigger actin polymerization even in the absence of phagocytic ligands. We speculate that this preassembly of actin polymers may accelerate the phagocytic process upon recognition of the foreign particle. Previous reports have shown actin polymerization after HS (34, 35) or GA treatment (36, 37). Hsp70 and Hsp90 have been shown to be recruited in close proximity to actin filaments and microtubules during stress conditions (38). The interaction of Hsp70 with tubulin, intermediate filaments, and microtubules has also been reported (39, 40). Hsp90 has been proposed to be involved in stabilization of the cytoskeleton due to its interaction with actin (41), tubulin (42), intermediary filaments (43), dynein (44), τ proteins (40), and calponin (45). Small Hsps, particularly Hsp27, have also been implicated in different aspects of actin polymerization (46, 47). Expression of Hsp27 was correlated with an increase in F-actin within plasma membrane ruffling, pinocytosis, and accumulation of stress fibers (46) as well as with enhanced endothelial cell migration (48). Moreover, it has been suggested that phosphorylated Hsp27 stabilizes the actin network at the base of lamellipodia (48, 49). Thus, it is likely that the expression of Hsps by inhibition of Hsp90 function (GA treatment) or after HS modulates cytoskeleton organization. This Hsp-related alteration of the cytoskeleton might be responsible, at least in part, for the increase in phagocytosis. Thus, higher rates of phagocytic vesicle formation or phagosome maturation may contribute to the acceleration of the phagocytic process. This assumption is consistent with our observations that neither binding of opsonized particles to the cell surface nor the presence of FcγRs on the plasma membrane was increased upon GA treatment. Moreover, no oxidative stress or NADPH oxidase activation was observed upon incubation with GA, suggesting that a ROS-related mechanism is not involved in the increase in phagocytosis.

In summary, our observations indicate that phagocytosis is enhanced during stressful conditions. This increase in phagocytosis may be due to more efficient engulfment or trafficking of the phagocytic vesicles, rather than to elevated binding of particles to the cell surface. In fact, we have previously shown that GA treatment of Mϕs resulted in accelerated disappearance of CD14 from the cell surface (27). GA treatment has also been associated with alterations in cellular trafficking of insulin receptor (50), epidermal growth factor receptor (51, 52), platelet-derived growth factor receptor, and pp60 (51). We speculate that the possible effect of Hsps on the increase in phagocytosis is part of the general response to stress. Thus, a rapid uptake of cell debris or necrotic cells formed after injury assures a reduction in damage propagation and control of the inflammatory response. The effective clearance of apoptotic cells avoids secondary complications due to postapoptotic necrosis. Moreover, this enhancement in phagocytosis during stress may play a role in the control of postinjury infections, which are the most common cause of secondary complications and mortality in trauma patients. Overall, this preactivation of professional phagocytes during the early stages of the stress response could be beneficial for preventing secondary complications and increasing prospects for survival after injury. Finally, our observations add phagocytosis to the large list of cellular processes that are potentially modulated by the presence of Hsps.

Acknowledgments

We thank Alejandro Barbieri, Ph.D., for his constructive comments. Michael Kalcevic's technical assistance with flow cytometric analysis is appreciated.

Disclosures

The authors have no financial conflict of interest.

References

1. Morimoto, R. I. 1991. Heat shock: the role of transient inducible responses in cell damage, transformation and differentiation. *Cancer Cells* 3: 295–301.
2. De Maio, A. 1999. Heat shock proteins: facts, thoughts, and dreams. *Shock* 11: 1–12.
3. Minowada, G., and W. J. Welch. 1995. Clinical implications of the stress response. *J. Clin. Invest.* 95: 3–12.
4. Nicchitta, C. V. 2003. Re-evaluating the role of heat-shock protein-peptide interactions in tumour immunity. *Nat. Rev. Immunol.* 3: 427–432.
5. Basu, S., R. J. Binder, R. Suto, K. M. Anderson, and P. K. Srivastava. 2000. Necrotic but not apoptotic cell death releases heat shock proteins, which deliver a partial maturation signal to dendritic cells and activate the NF-κB pathway. *Int. Immunol.* 12: 1539–1546.
6. Whitesell, L., E. G. Mimnaugh, B. De Costa, C. E. Myers, and L. M. Neckers. 1994. Inhibition of heat shock protein HSP90-pp60v-src heteroprotein complex formation by benzoquinone ansamycins: essential role for stress proteins in oncogenic transformation. *Proc. Natl. Acad. Sci. USA* 91: 8324–8328.
7. Zou, J., Y. Guo, T. Guettouche, D. F. Smith, and R. Voellmy. 1998. Repression of heat shock transcription factor HSF1 activation by HSP90 (HSP90 complex) that forms a stress-sensitive complex with HSF1. *Cell* 94: 471–480.
8. Morimoto, R. I. 1998. Regulation of the heat shock transcriptional response: cross talk between a family of heat shock factors, molecular chaperones, and negative regulators. *Genes Dev.* 12: 3788–3796.
9. Antoni, F. A. 1986. Hypothalamic control of adrenocorticotropin secretion: advances since the discovery of 41-residue corticotropin-releasing factor. *Endocr. Rev.* 7: 351–378.
10. Sapolsky, R. M. 2000. Stress hormones: good and bad. *Neurobiol. Dis.* 7: 540–542.
11. Laroux, F. S. 2004. Mechanisms of inflammation: the good, the bad and the ugly. *Front. Biosci.* 9: 3156–3162.
12. Araki, N., M. T. Johnson, and J. A. Swanson. 1996. A role for phosphoinositide 3-kinase in the completion of macropinocytosis and phagocytosis by macrophages. *J. Cell Biol.* 135: 1249–1260.
13. Ghazizadeh, S., J. B. Bolen, and H. B. Fleit. 1994. Physical and functional association of Src-related protein tyrosine kinases with FcγRII in monocytic THP-1 cells. *J. Biol. Chem.* 269: 8878–8884.
14. Strzelecka-Kiliszek, A., K. Kwiatkowska, and A. Sobota. 2002. Lyn and Syk kinases are sequentially engaged in phagocytosis mediated by FcγR. *J. Immunol.* 169: 6787–6794.
15. Hackam, D. J., O. D. Rotstein, A. Schreiber, W. Zhang, and S. Grinstein. 1997. Rho is required for the initiation of calcium signaling and phagocytosis by Fcγ receptors in macrophages. *J. Exp. Med.* 186: 955–966.
16. Brumell, J. H., and S. Grinstein. 2003. Role of lipid-mediated signal transduction in bacterial internalization. *Cell. Microbiol.* 5: 287–297.
17. Vieira, O. V., R. J. Botelho, and S. Grinstein. 2002. Phagosome maturation: aging gracefully. *Biochem. J.* 366: 689–704.
18. Lennartz, M. R. 1999. Phospholipases and phagocytosis: the role of phospholipid-derived second messengers in phagocytosis. *Int. J. Biochem. Cell Biol.* 31: 415–430.
19. Tjelle, T. E., T. Lovdal, and T. Berg. 2000. Phagosome dynamics and function. *BioEssays* 22: 255–263.
20. Botelho, R. J., C. C. Scott, and S. Grinstein. 2004. Phosphoinositide involvement in phagocytosis and phagosome maturation. *Curr. Top. Microbiol. Immunol.* 282: 1–30.
21. Howard, T. H., and C. O. Oresajo. 1985. The kinetics of chemotactic peptide-induced change in F-actin content, F-actin distribution, and the shape of neutrophils. *J. Cell Biol.* 101: 1078–1085.
22. Feinberg, A. P., and B. Vogelstein. 1983. A technique for radiolabeling DNA restriction endonuclease fragments to high specific activity. *Anal. Biochem.* 132: 6–13.
23. Beck, C. S., and A. De Maio. 1994. Stabilization of protein synthesis in thermotolerant cells during heat shock: association of heat shock protein-72 with ribosomal subunits of polysomes. *J. Biol. Chem.* 269: 21803–21811.
24. Ellman, G., and H. Lysko. 1979. A precise method for the determination of whole blood and plasma sulfhydryl groups. *Anal. Biochem.* 93: 98–102.

25. Sittler, A., R. Lurz, G. Lueder, J. Priller, H. Lehrach, M. Hayer-Hartl, F. Hartl, and E. Wanker. 2001. Geldanamycin activates a heat shock response and inhibits huntingtin aggregation in a cell culture model of Huntington's disease. *Hum. Mol. Genet.* 10: 1719.
26. Bagatell, R., G. Paine-Murrieta, C. Taylor, E. Pulcini, S. Akinaga, I. Benjamin, and L. Whitesell. 2000. Induction of a heat shock factor 1-dependent stress response alters the cytotoxic activity of hsp90-binding agents. *Clin. Cancer Res.* 6: 3312–3318.
27. Vega, V. L., and A. De Maio. 2003. Geldanamycin treatment ameliorates the response to LPS in murine macrophages by decreasing CD14 surface expression. *Mol. Biol. Cell.* 14: 764–773.
28. Dikalov, S., U. Landmesser, and D. G. Harrison. 2002. Geldanamycin leads to superoxide formation by enzymatic and non-enzymatic redox cycling: implications for studies of Hsp90 and endothelial cell nitric-oxide synthase. *J. Biol. Chem.* 277: 25480–25485.
29. Lai, M. T., K. L. Huang, W. M. Chang, and Y. K. Lai. 2003. Geldanamycin induction of grp78 requires activation of reactive oxygen species via ER stress responsive elements in 9L rat brain tumour cells. *Cell. Signal.* 15: 585–595.
30. Ueyama, T., M. R. Lennartz, Y. Noda, T. Kobayashi, Y. Shirai, K. Rikitake, T. Yamasaki, S. Hayashi, N. Sakai, H. Seguchi, et al. 2004. Superoxide production at phagosomal cup/phagosome through βI protein kinase C during FcγR-mediated phagocytosis in microglia. *J. Immunol.* 173: 4582–4589.
31. Welch, W. J., and J. P. Suhan. 1985. Morphological study of the mammalian stress response: characterization of changes in cytoplasmic organelles, cytoskeleton, and nucleoli and appearance of intranuclear actin filaments in rat fibroblasts after heat-shock treatment. *J. Cell Biol.* 101: 1198–1211.
32. Arispe, N., M. Doh, and A. De Maio. 2002. Lipid interaction differentiates the constitutive and stress-induced heat shock proteins Hsc70 and Hsp70. *Cell Stress Chaperones* 7: 330–338.
33. Arispe, N., M. Doh, O. Simakova, B. Kurganov, and A. De Maio. 2004. Hsc70 and Hsp70 interact with phosphatidylserine on the surface of PC12 cells resulting in a decrease of viability. *FASEB J.* 18: 1636–1645.
34. Collier, N. C., and M. J. Schlesinger. 1986. The dynamic state of heat shock proteins in chicken embryo fibroblasts. *J. Cell Biol.* 103: 1495–1507.
35. Han, S. I., K. S. Ha, K. I. Kang, H. D. Kim, and H. S. Kang. 2000. Heat shock-induced actin polymerization, SAPK/JNK activation, and heat-shock protein expression are mediated by genistein-sensitive tyrosine kinase(s) in K562 cells. *Cell Biol. Int.* 24: 447–457.
36. Sreedhar, A. S., K. Mihaly, B. Pato, T. Schnaider, A. Stetak, K. Kis-Petik, J. Fidy, T. Simonics, A. Maraz, and P. Csermely. 2003. Hsp90 inhibition accelerates cell lysis: anti-Hsp90 ribozyme reveals a complex mechanism of Hsp90 inhibitors involving both superoxide- and Hsp90-dependent events. *J. Biol. Chem.* 278: 35231–35240.
37. Pai, K. S., V. B. Mahajan, A. Lau, and D. D. Cunningham. 2001. Thrombin receptor signaling to cytoskeleton requires Hsp90. *J. Biol. Chem.* 276: 32642–32647.
38. Kirby, B. A., C. R. Merril, H. Ghanbari, and W. C. Wallace. 1994. Heat shock proteins protect against stress-related phosphorylation of tau in neuronal PC12 cells that have acquired thermotolerance. *J. Neurosci.* 14: 5687–5693.
39. Liao, J., L. A. Lowthert, N. Ghori, and M. B. Omary. 1995. The 70-kDa heat shock proteins associate with glandular intermediate filaments in an ATP-dependent manner. *J. Biol. Chem.* 270: 915–922.
40. Dou, F., W. J. Netzer, K. Tanemura, F. Li, F. U. Hartl, A. Takashima, G. K. Gouras, P. Greengard, and H. Xu. 2003. Chaperones increase association of τ protein with microtubules. *Proc. Natl. Acad. Sci. USA* 100: 721–726.
41. Kellermayer, M. S., and P. Csermely. 1995. ATP induces dissociation of the 90 kDa heat shock protein (hsp90) from F-actin: interference with the binding of heavy meromyosin. *Biochem. Biophys. Res. Commun.* 211: 166–174.
42. Williams, N. E., and E. M. Nelsen. 1997. HSP70 and HSP90 homologs are associated with tubulin in hetero-oligomeric complexes, cilia and the cortex of *Tetrahymena*. *J. Cell Sci.* 110: 1665–1672.
43. Czar, M. J., M. J. Welsh, and W. B. Pratt. 1996. Immunofluorescence localization of the 90-kDa heat-shock protein to cytoskeleton. *Eur. J. Cell Biol.* 70: 322–330.
44. Galigniana, M. D., J. M. Harrell, P. J. Murphy, M. Chinkers, C. Radanyi, J. M. Renoir, M. Zhang, and W. B. Pratt. 2002. Binding of hsp90-associated immunophilins to cytoplasmic dynein: direct binding and in vivo evidence that the peptidylprolyl isomerase domain is a dynein interaction domain. *Biochemistry* 41: 13602–13610.
45. Ma, Y., N. V. Bogatcheva, and N. B. Gusev. 2000. Heat shock protein (hsp90) interacts with smooth muscle calponin and affects calponin-binding to actin. *Biochim. Biophys. Acta* 1476: 300–310.
46. Lavoie, J. N., G. Gingras-Breton, R. M. Tanguay, and J. Landry. 1993. Induction of Chinese hamster HSP27 gene expression in mouse cells confers resistance to heat shock: HSP27 stabilization of the microfilament organization. *J. Biol. Chem.* 268: 3420–3429.
47. Piotrowicz, R. S., and E. G. Levin. 1997. Basolateral membrane-associated 27-kDa heat shock protein and microfilament polymerization. *J. Biol. Chem.* 272: 25920–25927.
48. Piotrowicz, R. S., E. Hickey, and E. G. Levin. 1998. Heat shock protein 27 kDa expression and phosphorylation regulates endothelial cell migration. *FASEB J.* 12: 1481–1490.
49. Pichon, S., M. Bryckaert, and E. Berrou. 2004. Control of actin dynamics by p38 MAP kinase: Hsp27 distribution in the lamellipodium of smooth muscle cells. *J. Cell Sci.* 117: 2569–2577.
50. Saitoh, T., T. Yanagita, S. Shiraishi, H. Yokoo, H. Kobayashi, S. Minami, T. Onitsuka, and A. Wada. 2002. Down-regulation of cell surface insulin receptor and insulin receptor substrate-1 phosphorylation by inhibitor of 90-kDa heat-shock protein family: endoplasmic reticulum retention of monomeric insulin receptor precursor with calnexin in adrenal chromaffin cells. *Mol. Pharmacol.* 62: 847–855.
51. Sakagami, M., P. Morrison, and W. J. Welch. 1999. Benzoquinoid ansamycins (herbimycin A and geldanamycin) interfere with the maturation of growth factor receptor tyrosine kinases. *Cell Stress Chaperones* 4: 19–28.
52. Supino-Rosin, L., A. Yoshimura, Y. Yarden, Z. Elazar, and D. Neumann. 2000. Intracellular retention and degradation of the epidermal growth factor receptor, two distinct processes mediated by benzoquinone ansamycins. *J. Biol. Chem.* 275: 21850–21855.